

Development of a distributed, fully automated, bidirectional telemetry system for amperometric microsensor and biosensor applications

Gaia Rocchitta^a, Rossana Migheli^a, Sonia Dedola^a, Giammaria Calia^a, Maria S. Desole^a, Egidio Miele^a, John P. Lowry^b, Robert D. O'Neill^c, Pier A. Serra^{a,*}

^a Department of Pharmacology, Medical School, University of Sassari, Viale S. Pietro 43/b, 07100 Sassari, Italy

^b Department of Chemistry, National University of Ireland, Maynooth, Co. Kildare, Ireland

^c UCD School of Chemistry and Chemical Biology, University College Dublin, Belfield, Dublin 4, Ireland

Received 1 March 2007; received in revised form 13 April 2007; accepted 13 April 2007

Available online 19 April 2007

Abstract

A new bidirectional telemetry system for amperometric sensor applications has been developed. A fully automated peripheral unit (PU), constituted by a potentiostat, a two-channel I/V converter, a microcontroller unit (MCU) and a signal transmitter, was designed, constructed, and tested. A peripheral interface controller (PIC) MCU drives a digital-to-analog converter (DAC), which polarized the sensor, while the resulting anodic current is converted to a digital value by an analog-to-digital converter (ADC). The PIC firmware is developed in assembly and transferred to the MCU through a bootloader algorithm. The digital data are sent to a personal computer using a 4-byte packet protocol by means of a miniaturized 433 MHz frequency modulation (FM) transceiver with a linear range up to 200 m. The central unit (CU) is connected to a PC via Universal Serial Bus (USB). Custom developed software, implemented in Basic and C, allows the PC to control several PUs and record, plot and handle received data. The development and operation of the hardware and software are described. The system performance was evaluated using an automated dummy cell connected to the PU. The amperometric response of nitric oxide (NO), dopamine (DA) microsensors and a glucose biosensor was determined *in vitro*. This apparatus serves as a basic model to realize an *in vivo* bidirectional telemetry system built with standard components readily available at low cost.

© 2007 Elsevier B.V. All rights reserved.

Keywords: Potentiostat; Amperometry; Microcontroller; Microsensor; Biosensor; Biotelemetry

1. Introduction

Medical telemetry may be defined as “the measurement and recording of physiological parameters and other patient-related information via radiated bi- or unidirectional electromagnetic signals” [1] or, simply, as the measurement of a biomedical parameter at a distance.

The most important aim of biotelemetry is the rapid recognition of significant changes in physiological parameters, such that therapeutic treatment can occur early [2]. This technique allows, for example, real-time reading of glucose levels in diabetic patients [3,4], critical care [5] and brain injuries [6]. In recent years sophisticated biotelemetry systems have been devel-

oped for research purposes to analyse neurochemical data such as brain variations of dopamine in freely moving animals [7–8]. Telemetric devices can be coupled with microsensors or biosensors that generate electrical signals related to electrochemical processes [9].

Several biologically oxidable molecules can be directly detected on the surface of amperometric sensors connected to a potentiostat [10]. The constant-potential oxidation of NO [11,12] and DA [13] occur on coated carbon fibers with a good selectivity against electrochemically oxidizable anions. When direct electrochemical oxidation of biological compounds is not possible in standard conditions, as in the case of glucose, a biosensor may then be used instead [14]. In this paper we describe a fully automated multi-channel biotelemetry system, derived from a previously published apparatus [15] which can be used with microsensors/biosensors for the measurement of NO, DA, glucose and other bio-

* Corresponding author. Tel.: +39 079 228558; fax: +39 079 228525.
E-mail address: paserra@uniss.it (P.A. Serra).

logically interesting molecules *in vitro* and potentially *in vivo*.

2. Experimental

2.1. Chemicals and solutions

All analytical grade chemicals were used as supplied and dissolved in MilliQ water. *S*-nitroso-*N*-acetylpenicillamine (SNAP), dopamine (DA), ascorbic acid (AA), Nafion® (5% in aliphatic alcohols) and sodium nitrite were purchased from Sigma–Aldrich (Milano, Italy). The stock solution of glucose (1 M) was prepared in water and stored at room temperature for 24 h to allow the equilibration of the two anomers, then used for calibration. The glucose oxidase (GOx) from *Aspergillus niger* (EC 1.1.3.4.), *o*-phenylenediamine (OPD) and D(+)-Glucose were obtained from Sigma Chemicals (Milano, Italy). The phosphate-buffer saline (PBS) solution was made using NaCl (137 mM), KCl (2.7 mM), NaH₂PO₄ (1.4 mM) and Na₂HPO₄ (4.3 mM) from Sigma, then adjusted to pH 7.4. The GOx solution was prepared by dissolving 448 units (2.5 mg) of enzyme in 25 μ L of PBS and then stored at 4 °C. The OPD monomer was dissolved in deoxygenated PBS immediately before the electrochemical synthesis of the polymer (poly-OPD, p-OPD) on carbon/Pt surface. The stock solutions of DA (250 μ M) and SNAP (1 mM) were freshly prepared in water immediately before use. The saturated solution of cuprous chloride was made by adding 150 mg CuCl to 500 mL deoxygenated water [11]. The

3 M NaOH solution for the development of the positive photoresist was prepared in 500 mL of water by dissolving 60 g of NaOH tablets (Sigma). The etching solution (FeCl₃, 2 M) was prepared dissolving 82 g of ferric chloride (Sigma) in 250 mL of water.

2.2. Materials and electronic parts

Electronic parts were from Farnell InOne spa (Milano, Italy); the radio modules were from Telecontrolli spa (TC, Casoria, Italy), and the USB components preassembled by Elettronicamente (ELT, Milano, Italy). The power section of the peripheral unit (PU) was stabilized using a National LP2950-05 voltage regulator. The amperometric section of the PU was built using two National-LMC6064 while the gain of the differentiators was controlled with four digital potentiometers (Microchip MCP-42100). The ADC–DAC system was built using Integrated circuits from Dallas–Maxim Semiconductors: MAX1270 (ADC), MAX5156 (DAC), MAX6126 (DAC- V_{Ref}). The MCUs used in the system were: a Microchip 16F876A in the PU and a Microchip 12F683 in the central unit (CU). The 433.33/433.92 MHz FM transmitters were RXQ1-433.9 (TC). The antennas (1/4 wavelength and compressed helical models) were from RF solutions (Northants, UK). The serial-to-USB converter used in the CU was a FTDI-FT232BM module (ELT) with a 6 MHz quartz and a 93C46 E²PROM. A CMOS HEX Inverter (74HCT04N, Philips Semiconductors) completed the CU. The dummy cell was built using one NUD3105D Inductive Load Driver (ON Semiconductor,

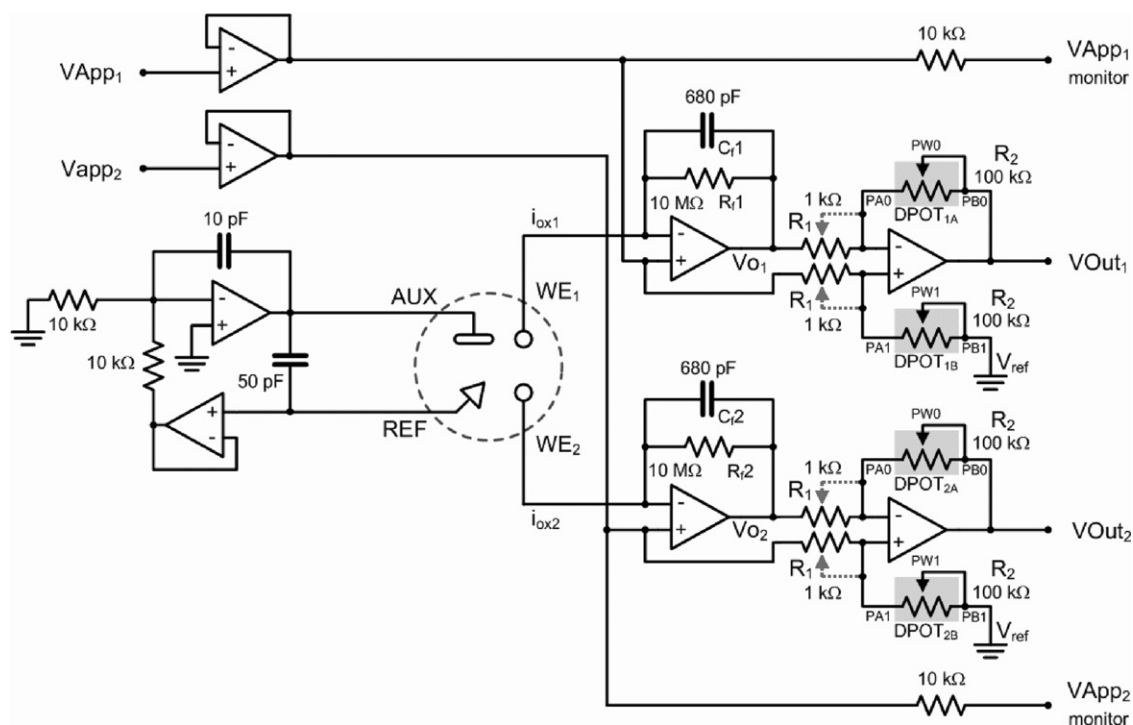


Fig. 1. Circuit diagram of the amperometric section of the peripheral unit. The system consists of two OPA potentiostat, two-channel buffered voltage follower, two current-to-voltage (I/V) converters and two programmable single-supply differentiators/amplifiers. The potential applied to the working electrodes (V_{App1} , V_{App2}) is generated by a two-channel DAC and monitored by the ADC. The I/V converters amplify the oxidation currents (i_{ox1-2}) with a fixed gain determined by the value of R_{f1} and R_{f2} . The differentiators/amplifiers, connected to MCU-driven digital potentiometers (DPOT_{1A-B}, DPOT_{2A-B}), perform the subtraction of the applied potential from the first stage of amplification (V_{O1-2}) and further amplify the signal. The resulting output voltage (V_{Out1} , V_{Out2}) is monitored by the ADC.

Phoenix, USA) and two 98-1-C-5/3D low-current reed relays (Pickering Electronics Limited, UK). All resistors were precision metal oxide thick film (1/4 W, 0.1% tolerance, Ohmite, Rolling Meadows, IL). All capacitors were NP0-type multilayer ceramic (low-pass filter, decoupling) or electrolytic (decoupling). The components were soldered on a single side PCB board (eurocard size—160 mm × 100 mm) and mounted in ABS electronic enclosures (45.5 mm H × 138 mm W × 190 mm D). The Power source of the PU was a Panasonic rechargeable 8.4 V Nickel–Metal hydride (Ni-Mh) battery pack (3300 mA/h). Emilac®, Positiv® and Plastic® technical sprays were from Cramolin (Mühlacker, Germany).

2.3. Peripheral unit circuit description

The PU (Fig. 2) comprised two different parts: the amperometric module and the digital module. The two-channel

amperometric section (Fig. 1; Fig. 2, light gray) was built around the integrated circuit (IC) LMC6044, a quad single-supply operational amplifier (OPA). This CMOS micropower IC can operate from a single-supply voltage with “Rail-to-Rail” inputs and outputs. The following description concerns a single analog channel. One OPA serves as voltage follower connected to the DAC. This circuit produces the voltage necessary to polarize the working electrode (WE) between 0 and +2 V in accord with the following equation:

$$V_{App} = \frac{V_{Ref} D_N}{2^N} \quad (1)$$

where V_{Ref} is the reference voltage generated by the MAX6126, D_N the numeric value of the MAX5156 binary input code (0–4095) and N is the number of DAC bits (12). A two OPA potentiostat controls the reference (RE) and the auxiliary (AE) electrodes. The current-to-voltage (I/V) converter is a single-supply adaptation of a classic transimpedance amplifier [16]

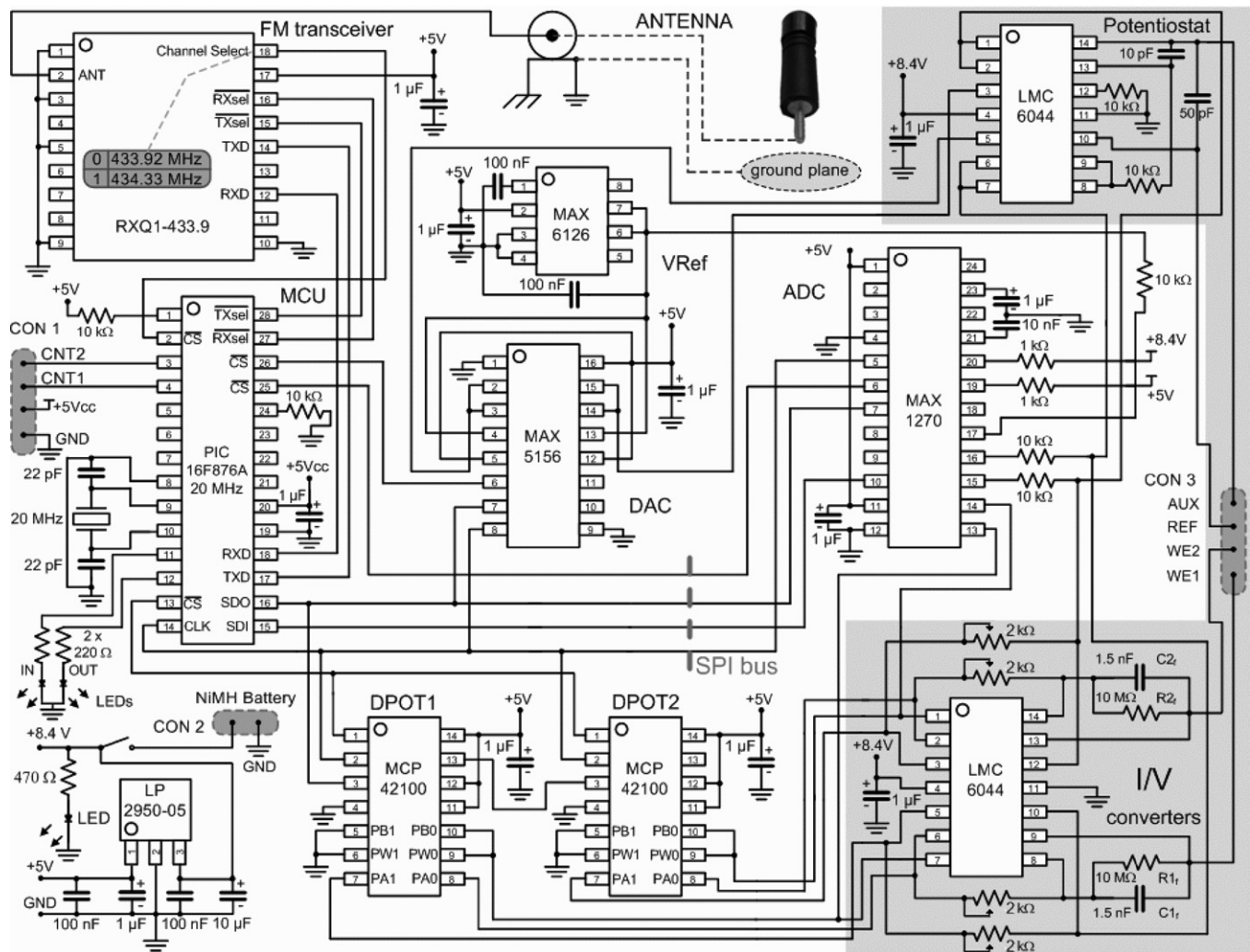


Fig. 2. Detailed circuit diagram of the peripheral unit (see text). The amperometric section (light gray) comprises a two-channel buffered voltage follower, a potentiostat, two current-to-voltage converters and two programmable single-supply differentiators/amplifiers. The +5 V voltage is stabilized by a low drop-out voltage regulator (LP2950-05). The programmable digital section is equipped with a PIC-16F876A MCU, working at 20 MHz, connected to a two-channel 12 bit DAC (MAX5156), a 8-channel 12-bit ADC (MAX1270) and two MCP42100 containing four 8-bit digital potentiometers. A precision voltage reference (MAX6126), connected to the DAC, completes the unit. The serial port of the MCU is directly wired to the FM transceiver (RXQ1-433.9). The firmware has been transferred via radio to the MCU (running a bootloader algorithm) through the central unit wired to a personal computer.

with a fixed gain. The transfer function of the I/V converter is:

$$V_O = -(i_{Ox} R_f) + V_{App} \quad (2)$$

where i_{Ox} is the oxidation current flowing through the WE, R_f the $10\text{ M}\Omega$ feedback resistor and V_{App} is the potential applied to the WE. The resistor has a capacitor in parallel to complete a low-pass filter with a cut-off frequency ($F_{\text{cut-off}}$) of 23.5 Hz. The capacitor value (C_f , 680 pF) was calculated in Farads according to the equation:

$$C_f = \frac{1}{F_{\text{cut-off}} 2\pi R_f} \quad (3)$$

The difference amplifier circuit has the dual role of subtracting the potential applied to the WE [15,16] while amplifying up to 100 times the resulting signal. The simplified DC transfer function of the differentiator is [17]:

$$V_{\text{Out}} = (V_O - V_{App}) \left(\frac{R_2}{R_1} \right) + V_{\text{ref}} \left(\frac{R_2}{R_1} \right) \quad (4)$$

where V_O and V_{App} are the signals applied to the inputs and R_1 and R_2 are respectively $1\text{ k}\Omega$ resistors and $100\text{ k}\Omega$ digital potentiometers (8 bit DPOTs, $390.625\ \Omega$ LSB) configured as rheostats. V_{ref} is equal to 0 V because R_2 is grounded, then:

$$V_{\text{Out}} = \left(\frac{R_2}{R_1} \right) (V_O - V_{App}) \quad (5)$$

The combination of the two stages of amplification provides up to 256 different full scales, according with the R_2 value, ranging from 1 nA/V up to 100 nA/V, with the global transfer function:

$$V_{\text{Out}} = - \left(\frac{R_2}{R_1} \right) (i_{Ox} R_f) \quad (6)$$

The value of R_2 was digitally defined as:

$$R_2 = \left(\frac{(100\text{ k}\Omega D_N)}{2^N} \right) + R_w \quad (7)$$

In which D_N is the 8-bit digital code (in decimal form) that is used to program the DPOT (0–255), N is the number of digital potentiometer bits (8) and R_w is the parasitic resistance through the wiper of the DPOT ($125\ \Omega$). The low tolerance resistors (0.1%) and the laser trimming process of production of the MCP42100 (mismatches between two internal potentiometers <0.2%) reduce the amplification error in the I/V design and the voltage-subtraction error in the differentiator circuit. With a power supply of +8.4 V and V_{App} fixed to +2.0 V, the maximum input current is almost 600 nA (620 nA in the observed “rail-to-rail” output). In this range of amplifications it is possible to calibrate accurately NO, DA and glucose microsensors/biosensors *in vitro*. The power supply was built using a LP2950-5.0, +5V voltage regulator, and two decoupling capacitors. This IC has very low quiescent current ($75\ \mu\text{A}$), low drop-out voltage (40–100 mV) and excellent linear regulation (0.05%).

The PIC16F876A is the core of the digital module (Fig. 2). This is a 8-bit CMOS IC with low power features. The MCU,

working at 20 MHz, controlled the ADC, the DAC and the daisy-chained DPOTs [18] using a SPI™ serial interface. After the digital signal processing (DSP) of acquired raw data, a data packet was generated and sent to the transmitter. A bootloader algorithm provides the possibility of programming the IC “on-board” in a few seconds.

The dual band FM transceiver is a thick film module with crystal controlled oscillator and external compressed helical antenna. The module contains two RF channels at 433.92 and 434.33 MHz selectable by firmware. In conjunction with the MCU, this hybrid component allows the realization of bidirectional data transfer devices, working at the maximum speed of 20 Kbaud, at ranges up to 200 m. The description of the automated two-channel dummy cell connected to PU and used for electronics calibrations can be found in supplementary material.

A rechargeable 8.4 V Nickel–Metal hydride (Ni-Mh) Battery pack (3300 mA/h) provided the power to the unit.

2.4. Central unit circuit description

The CU (Fig. 3), mapped as “Zero Unit”, comprises two parts: the microcontrolled-driven transceiver (TX-RX) module and the serial-to-USB converter. The MCU (12F683, running at 8 MHz), has the main role of changing the carrier frequency of the FM module, switching between RX and TX modes (74HCT04N) and permitting the remote control of multiple peripheral units. The RXQ1-433.9 is the same described in the PU. An external antenna, consisting of one quarter of wavelength ($\lambda/4$) plastic-coated straight wire, was connected directly to the antenna pin of the transceiver (Fig. 4).

The TX-RX module transmitted the digital data to the Serial-to-USB converter (Fig. 3, light gray). This hardware section was built around the FT232BM, clocked at 6 MHz and connected to an external 93C46 E²PROM (used to store USB ID parameters, resource configuration, etc.). Two LEDs provided direct visualization of IN–OUT data packets. A few resistors and decoupling capacitors completed the USB interface and the +5 V power supply, derived from the USB. PCB design and construction can be found in supplementary material.

2.5. Preparation and calibration of NO and DA microsensors and glucose biosensor

NO microsensors were built modifying a procedure previously described [19–21]. Briefly, a carbon fibre electrode ($\varnothing = 30\ \mu\text{m}$; length = $\sim 500\ \mu\text{m}$) was modified with poly-*O*-phenylenediamine (using OPD monomer, 250 mM) and Nafion® (3 coats). After p-OPD and Nafion® treatment, only electrodes with NO detection limits <50 nM and selectivity against ascorbic acid (AA; >1000:1), DA (>250:1), and nitrite (>800:1) were used. The calibration of selective NO microelectrodes was performed by adding known volumes of a standard SNAP solution in a saturated CuCl solution [11], DA microsensors ($\varnothing = 30\ \mu\text{m}$; length = $\sim 500\ \mu\text{m}$) were constructed similarly to those described by Yavich and Tiisonen [13] and tested for selectivity (DA:AA >1000:1). Platinum disk (5T-125 μm diameter, Advent Research Materials, Suffolk, UK) glucose biosensors

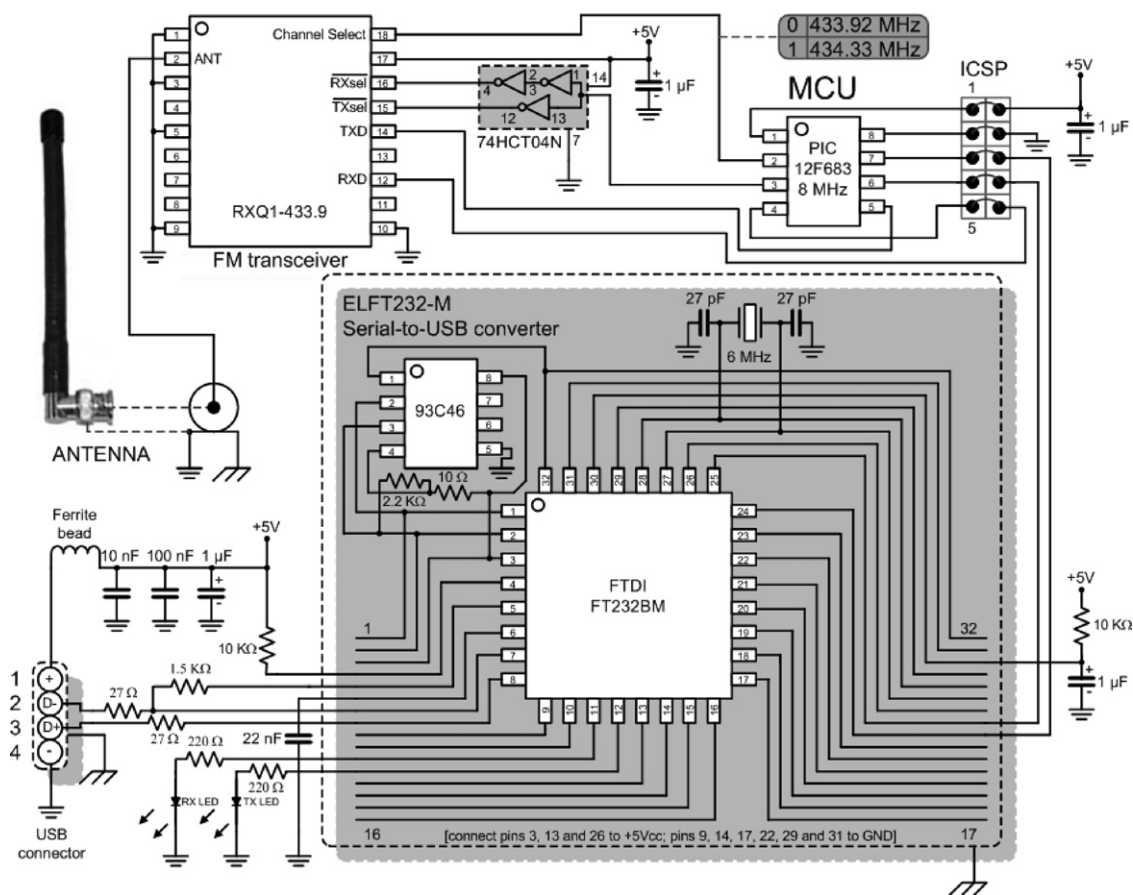


Fig. 3. Central unit: detailed circuit diagram (see text). The FM signal is encoded/decoded by the transceiver IC (RXQ1-433.9) connected to an external antenna. The bidirectional serial stream, filtered by the MCU (12F683) running at 8 MHz, is driven by a personal computer using a serial-to-USB converter (light gray). The MCU, mapped as “Zero Unit”, has the main role of changing the carrier frequency of the FM module, switching between RX and TX modes (74HCT04N) and permitting the remote programming of multiple peripheral units. The central unit has been programmed using an ICSP and is powered by the USB without the necessity of using an external power supply.

were prepared as previously described [15,22]. The electrosynthesis of p-OPD was performed at +700 mV in nitrogenated PBS. The reference and auxiliary electrodes were respectively an Ag/AgCl electrode and a 50 mm Platinum Wire (BAS-Bioanalytical Systems Inc., West Lafayette, US). All the *in vitro* calibrations were carried out at room temperature, using a custom made electrochemical cell [15], 24 h after the sensors had been manufactured. The electrodes were placed in the cell containing 20 mL of air-bubbled PBS (DA and glucose) or nitrogenated CuCl (NO). A positive potential (+865 mV for NO, +500 mV for DA and +700 mV for glucose) vs Ag/AgCl reference electrode was applied and the current recorded until a stable baseline was achieved. The calibrations were made and NO, DA and glucose curves were obtained in the range of concentrations illustrated in Fig. 6.

3. Results

3.1. Electronics test and calibration

The electronics of the PU was calibrated daily for three consecutive days. The automated two-channel dummy cell, described in supplementary material, was used as a double

Thevenin current source connected to the amperometric module. The voltage applied to a single channel of the dummy cell was generated between the WE and the AE/RE electrodes by the DAC of the PU and is equal to the voltage applied to the WE:

$$I_{\text{Dummy}} = \frac{V_{\text{App}}}{R_{\text{Dummy}}} \quad (9)$$

The resulting anodic current (i_{Dummy}) was read by the WE and converted in the resulting voltage (Eq. (6), V_{Out}) by the amperometric module.

The value of R_2 was digitally programmed to adjust the gain of the differentiator in the range comprised between 1 V/V and 100 V/V. From Eq. (6), R_2 (k Ω) was empirically calculated as follows:

$$R_2 = \frac{V_{\text{Out}}}{I_{\text{Dummy}} R_f} \times 1000 \quad (10)$$

where V_{Out} was fixed to 1 V and i_{Dummy} and R_f were respectively expressed in nA and M Ω . For example, a value of R_2 equal to 25 k Ω adjusts the amplification to 4 nA/V.

A 5-point calibration was made indoor for each of the seven amplification ranges with a linear distance between the peripherals and central units of ~ 25 m. Test conditions and experimental

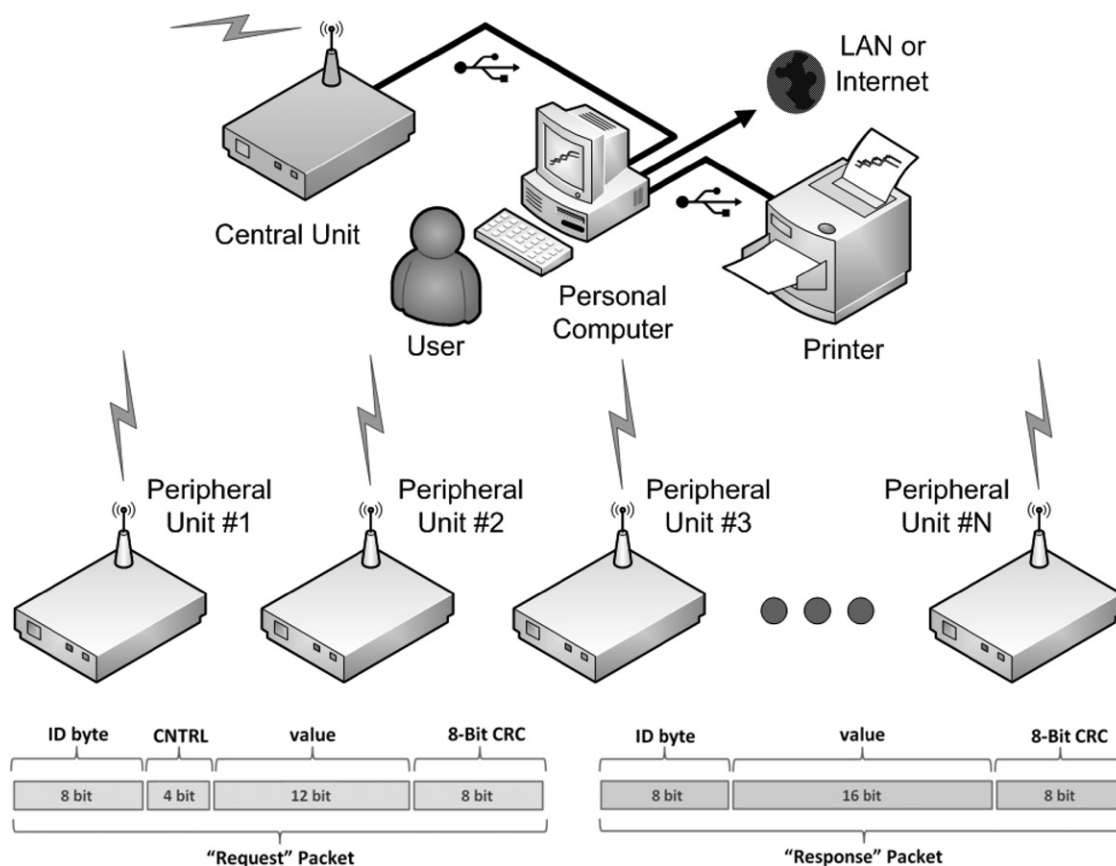


Fig. 4. Schematic representation of the system proposed in this study. A telemetric central unit (CU), physically wired to an Universal Serial Bus (USB), connects up to 255 peripheral units (PU) to a personal computer. Each PU can communicate with the CU using a half-duplex telemetry protocol consisting of four-bytes “Request” and “Response” data packets (see text). A custom developed software, able to drive the units, plot and store acquired data, interfaces the hardware with a printer (via USB), a Local Area Network (LAN) and Internet (via TCP/IP).

results are summarized in Table 1 while the logarithmic plot in Fig. 5 represents the calibration currents for each amplification range. The system shows excellent linearity across its entire range (Table 1, r^2 of recorded outputs >0.999). A second set of calibrations was made in the same conditions, connecting the V_{Out} of the amperometric module to a Fluke 45 voltmeter. No significant statistical differences were observed between the two calibrations (data not shown). After the operations described above, a 2.5 nA current was generated through the dummy cell, setting the R_{Dummy} to 100 M Ω and R_2 to 100 k Ω and fixing V_{App} to +250 mV. The system was left under these conditions up to the next calibration which was made the following day. A max-

imum V_{App} shift of ~ 10 mV was observed overnight while the current of the baseline noise was around 15 pA. Power results can be found in supplementary material.

3.2. Microsensors/biosensors response to DA, NO and glucose

NO generation from SNAP decomposition in saturated CuCl at 37 $^{\circ}\text{C}$ was measured according to Zhang et al. [11]. NO microsensors (Fig. 6, panel A; $n=6$) displayed good linearity ($r^2=0.997$) in the range of 0–11 μM with a slope of 0.37 ± 0.007 nA μM^{-1} . The calibration of DA microsen-

Table 1

Test conditions and experimental results of the peripheral unit calibration made by connecting the dummy cell and using it as a Thevenin current source (see text)

R_{Dummy} (M Ω)	V_{App} range (mV)	V_{app} step (mV)	Current range (nA)	DPOT R_2 value (K Ω)	Theoretical output (nA V^{-1})	Recorded output slope \pm S.E.M. (nA V^{-1})	Recorded output (r^2)
100	0–500	100	0–5	100	1	1.006 ± 0.009	0.9996
100	0–1000	200	0–10	50	2	2.044 ± 0.018	0.9991
100	0–2000	400	0–20	25	4	4.061 ± 0.032	0.9998
5	0–250	50	0–62.5	8	12.5	12.57 ± 0.125	0.9996
5	0–500	100	0–125	4	25	24.85 ± 0.089	0.9999
5	0–1000	200	0–250	2	50	50.26 ± 0.065	0.9999
5	0–2000	400	0–500	1	100	100.7 ± 0.322	0.9998

Each row represents a calibration curve ($n=6$) obtained using a predefined set of parameters. The full plot of calibration results is given in Fig. 5.

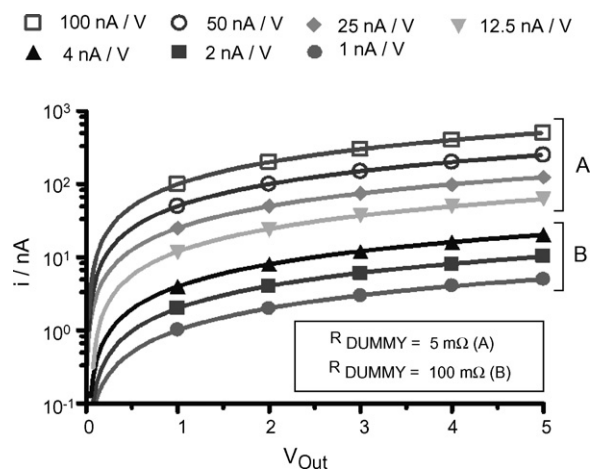


Fig. 5. Calibration of the peripheral unit by connecting the dummy cell and using it as a Thevenin current source (see text). Selecting the right R_{Dummy} value ($5\text{ M}\Omega$ or $100\text{ M}\Omega$) and applying a known voltage (V_{App}), a 5-point calibration was performed ($n=6$) for each amplification range. The logarithmic graph represents the calibration currents plotted vs. the output voltage of the differentiator (V_{Out}). Seven ranges of amplification were obtained changing the value of R_2 in the second stage of amplification: $1\text{ k}\Omega$ (100 nA/V), $2\text{ k}\Omega$ (50 nA/V), $4\text{ k}\Omega$ (25 nA/V), $8\text{ k}\Omega$ (12.5 nA/V), $25\text{ k}\Omega$ (4 nA/V), $50\text{ k}\Omega$ (2 nA/V) and $100\text{ k}\Omega$ (1 nA/V). The detailed description of experimental conditions and calibration results are given in Table 1.

sors (Fig. 6, panel B; $n=6$) was made in PBS ($0\text{--}2.75\text{ }\mu\text{M}$) obtaining a slope of $0.98 \pm 0.006\text{ nA }\mu\text{M}^{-1}$ ($r^2=0.999$). The *in vitro* response to glucose (Fig. 6, panel C) of p-OPD-based biosensors ($n=6$) in the range between 0 and 140 mM showed classical Michaelis–Menten kinetics ($r^2=0.955$). The values of V_{max} and K_m were respectively $68.9 \pm 2.4\text{ nA}$ and $5.72 \pm 0.96\text{ mM}$. The response to low concentrations of glucose ($0\text{--}2\text{ mM}$) showed a good linearity ($r^2=0.996$) with a slope of $10.83 \pm 0.35\text{ nA mM}^{-1}$.

4. Discussion

4.1. Operation and performance of the PU amperometric module

The amperometric module of the PU was optimized for single-supply, low-voltage operation, by distributing of the gain between the first and the second stage of amplification. Compared to our previous device [15] the gain selector was transferred from the I/V converter to the differentiator fixing R_f to $10\text{ M}\Omega$ while a double digital potentiometer controlled the amplification factor. Setting the R_2 value to $1\text{ k}\Omega$ (1 V/V gain) and V_{App} to 2 V , a maximum voltage output of 8.2 V was achieved from the first stage of amplification without the saturation of the second stage ($\sim 620\text{ nA}$ full scale).

The “rail-to-rail” output of the differentiator circuit, V_{Out} , corresponds to $R_2\text{ k}\Omega$ times the V_{app} -subtracted input signal (V_0). V_{Out} varies between 0 and $+8.2\text{ V}$. The limitations of this design are related to variations of the resistor values, mainly in the difference circuit [17].

The resistance variation of MCP42100 digital potentiometers is dependent on the construction process. The part-to-part

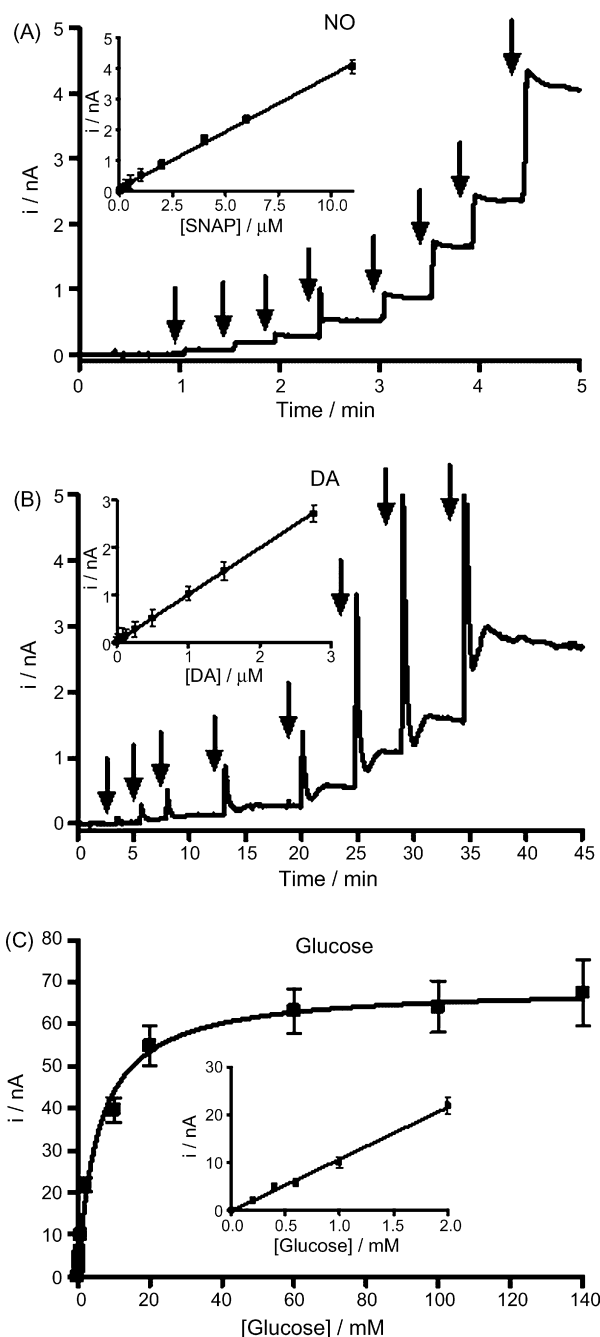


Fig. 6. *In vitro* calibration of NO and dopamine microsensors and a glucose biosensor connected to the peripheral unit at room temperature ($25\text{ }^\circ\text{C}$). Eight successive injections of SNAP (A) were made in a saturated CuCl solution in a range of concentrations between 0 and $11\text{ }\mu\text{M}$. The NO microsensor revealed good linearity ($r^2=0.997$, $n=6$) with a slope of $0.37 \pm 0.007\text{ nA }\mu\text{M}^{-1}$ (see A, inset). The calibration of DA microsensors (B, $n=6$) was made in PBS ($0\text{--}2.75\text{ }\mu\text{M}$) resulting in a slope of $0.98 \pm 0.006\text{ nA }\mu\text{M}^{-1}$ ($r^2=0.999$; see B, inset). Ten successive injections of glucose ($0.2, 0.4, 0.6, 1, 2, 10, 20, 60, 100, 140\text{ mM}$) were made in PBS. The calibration curve (panel C) showed classical Michaelis–Menten kinetics ($r^2=0.955$, $n=6$) with a V_{max} of $68.9 \pm 2.40\text{ nA}$ and a K_m of $5.72 \pm 0.96\text{ mM}$. The response to low concentrations of glucose ($0\text{--}2\text{ mM}$; C, inset) revealed good linearity ($r^2=0.996$) with a slope of $10.83 \pm 0.35\text{ nA mM}^{-1}$.

variation of the nominal resistance is quite large and is defined within a specified percentage ($100\text{ k}\Omega \pm 30\%$). However, the dual potentiometer can be used in the rheostat mode with a very high degree of precision [17] because the nominal resistances between the two internal potentiometers, in a single MCP42100 part, are ratio matched to a very small percentage ($<0.2\%$). The common-mode rejection (CMR) error, that is attributed to resistor mismatches, is demonstrated with a 12-bit, 5 V system, with a gain of 100 V/V, the common-mode voltage (CMV) ranges 0–5 V and the R_2 matching error is $\pm 0.2\%$. The error of this type of common-mode excursion is equal to 0.2 mV: five times less than 1 LSB [17]. Therefore, assuming a fixed value of R_1 ($1\text{ k}\Omega \pm 0.1\%$), the only true limitation in the differentiator circuit is the variation of the gain ($\pm 30\%$). Waiting for less part-to-part resistance variation of DPOTs, we solved this problem by changing the resistors R_1 with $2\text{ k}\Omega - 25$ turns – trimmer potentiometers (Figs. 1 and 2) to adapt R_1 ($1\text{ k}\Omega \pm 30\%$) to the measured value of R_2 [23]. The result is that the module is characterized by gain precision, stability and an excellent linear response (Table 1; Fig. 5). The system can operate only in oxidation mode and it is particularly suited to work in conjunction with direct-oxidation microsensors and biosensors with H_2O_2 detection as illustrated in Fig. 6. An alternative “attenuator” configuration, without advantages for our purposes, is possible when the R_2/R_1 ratio is lower than one.

4.2. Digital modules and wireless data transmission

The PIC16F876A, present in the PU, serves as DSP, serial transceiver and controls the DAC, the ADC and the dummy cell. In conjunction with the FM module, a complete digital wireless system has been implemented and the CRC calculation guarantees an optimal error check. Up to 255 PUs, with a 8 bit ID memorized in their E^2PROM , can share the same transmission channel but only one PU at a time can access it (half-duplex). The transmission protocol, consisting of 4-byte packets, permits the addressing of each PU. A two packet CU-PU exchange is the basic “Request-Response” transmission unit used during tests and calibrations. If the channel is noisy, it is possible to switch the modulation frequency.

The CU was interfaced to the software via USB with the possibility of high-level access to the received packets. This means that simple data capture and handling with popular software packages such as LabView[®] or DasyLab[®] is possible. Further details concerning firmware and software can be found in supplementary material. All experiments were made indoor and no communication problems were observed modifying the transmission distance in a linear range between 0 and 30 m. The 25 Hz sample rate is sufficient to detect sub-second variations of oxidation current compared with previous studies [4,7,8]. In addition, the 16F876A DSP improves the system performance.

4.3. Further development and future applications

In the present study we propose a wireless system based on discrete components and pre-built critical modules (FM transceiver, USB-interface), available at low cost, so no complex

hardware calibrations are needed. The system developed is similar to that previously described [15] with several improvements such as automatic gain control, electronics self test using dummy cell and bidirectional FM telemetry. The bidirectional telemetry, in particular, allowed the implementation of the distributed channel-sharing net. With a focused firmware development, several electrochemical techniques (chronoamperometry, differential pulse voltammetry, linear sweep voltammetry, etc.) can be integrated in the PU to extend the analytical capabilities of the system. Slow sweep voltammetry, for example, can be used for the long-term monitoring of brain DA metabolism using implanted carbon paste electrodes [24].

Experiments are in progress using XBee-PRO[™] modules (ZigBee[™], ZigBee Alliance) to obtain an increase in the serial data stream up to 115000 bps and the frequency to 2.4 GHz. A further hardware development comprises the integration of circuitry similar to the dummy cell in the PU for adjusting the I/V gain and low-pass filter. The *in vitro* characteristics of the proposed system justifies additional studies in order to monitor NO, DA and glucose levels in the brain of freely moving animals, but also other molecules present in the extracellular brain compartment such as lactate, ascorbic acid and glutamate [25].

5. Conclusion

In this article we have described the development of a distributed, fully automated, bidirectional telemetry system for amperometric microsensor/biosensor applications. The peripheral and the central units, based on simple and inexpensive components, can be successfully used for accurate transduction of the anodic currents generated on the surface of the sensors. At this stage of development the system exhibits high stability and excellent linear responses in the nanoampere current range. The choice of low power CMOS technology makes the project suitable of further improvements such as the reduction of the power consumption. The use of SM components and careful PCB design will make it possible to miniaturize the circuitry and to assemble a peripheral unit suitable for *in vivo* applications.

Acknowledgements

The authors acknowledge the Italian distributors of Microchip, Dallas–Maxim and National corporations for free samples of integrated circuits and Telecontrolli s.p.a. for the kind gift of miniaturized transceivers. The research was supported by University of Sassari (ex 60% fund).

Appendix A. Supplementary data

Supplementary data associated with this article can be found, in the online version, at doi:10.1016/j.snb.2007.04.019.

References

- [1] FCC, (Federal Communication Commission) (U.S.A.), Commission’s Rules to Create a Wireless Medical Telemetry Service, Document FCC 00-211, Washington, DC, June 8, 2000.

- [2] D.C. Leuher, Overview of biomedical telemetry techniques, *Eng. Med. Biol.* 3 (1983) 17–24.
- [3] M. Shichiri, N. Asasawa, Y. Yamasaki, R. Kawamori, H. Abe, Telemetry glucose monitoring device with needle glucose sensor: a useful tool for blood glucose monitoring in diabetic individuals, *Diabetes Care* 9 (1986) 298–301.
- [4] J. Black, M. Wilkins, P. Atanasov, E. Wilkins, Integrated sensor telemetry system for in vivo glucose monitoring, *Sens. Actuators B: Chem.* 31 (1996) 147–153.
- [5] N. Martin, Telemetry monitoring in acute and critical care, *Crit. Care Nurs. Clin. North Am.* 11 (1999) 77–85.
- [6] P.G. Matz, Monitoring in traumatic brain injury, *Clin. Neurosurg.* 44 (1997) 267–294.
- [7] F. Crespi, D. D'alessandro, V. Annovazzi-Lodi, C. Heibredner, M. Norgia, In vivo voltammetry: from wire to wireless measurements, *J. Neurosci. Methods* 140 (2004) 153–161.
- [8] P.A. Garris, R. Enzman, J. Poehlman, A. Alexander, P.E. Langley, S.G. Sandberg, P.G. Greco, R.M. Wightman, G.V. Rebec, Wireless transmission of fast-scan cyclic voltammetry at a carbon-fiber microelectrode: proof of principle, *J. Neurosci. Methods* 140 (2004) 103–115.
- [9] K.S. Yun, J. Gil, J. Kim, H.J. Kim, K. Kim, D. Park, M.S. Kim, H. Shin, K. Lee, J. Kwak, E. Yoon, A miniaturized low-power wireless remote environmental monitoring system based on electrochemical analysis, *Sens. Actuators B: Chem.* 102 (2004) 27–34.
- [10] A.J. Bard, L.R. Faulkner, *Electrochemical Methods: Fundamentals and Applications*, John Wiley & Sons, New York, 1980.
- [11] X. Zhang, L. Cardosa, M. Broderick, H. Fein, I.R. Davis, A novel method to calibrate nitric oxide microsensors by stoichiometrical generation of nitric oxide from SNAP, *Electroanalysis* 12 (2000) 425–428.
- [12] X. Zhang, Y. Kislyak, J. Lin, A. Dickson, L. Cardosa, M. Broderick, H. Fein, Nanometer size electrode for nitric oxide and *S*-nitrosothiols measurement, *Electrochem. Commun.* 4 (2002) 11–16.
- [13] L. Yavich, J. Tiihonen, In vivo voltammetry with removable carbon fibre electrodes in freely-moving mice: dopamine release during intracranial self-stimulation, *J. Neurosci. Methods* 104 (2000) 55–63.
- [14] P. Pantano, W.G. Kuhr, *Electroanalysis* 7 (1995) 405.
- [15] P.A. Serra, G. Rocchitta, G. Bazzu, A. Manca, G.M. Puggioni, J.P. Lowry, R.D. O'Neill, Design and construction of a low cost single-supply embedded telemetry system for amperometric biosensor applications, *Sens. Actuators B: Chem.* 1 (2007) 118–126.
- [16] J. Millar, J.J. O'Connor, S.J. Trout, Z.L. Kruk, Continuous scan cyclic voltammetry (CSCV): a new high-speed electrochemical method for monitoring neuronal dopamine release, *J. Neurosci. Methods* 43 (1992) 109–118.
- [17] B.C. Backer, Optimizing Digital Potentiometer Circuits to Reduce Absolute and Temperature Variations, Application Note AN691, Document DS00691A, Microchip Technology Inc., 2001.
- [18] C.L. King, E. Haile, Communicating with Daisy Chained MCP42XXX Digital Potentiometers, Application Note AN747, Document DS00747A, Microchip Technology Inc., 2001.
- [19] G. Rocchitta, R. Migheli, M.P. Mura, G. Esposito, M.S. Desole, E. Miele, M. Miele, P.A. Serra, Signalling pathways in the nitric oxide donor-induced dopamine release in the striatum of freely moving rats: evidence that exogenous nitric oxide promotes Ca^{2+} entry through store-operated channels, *Brain Res.* 1023 (2004) 243–252.
- [20] G. Rocchitta, R. Migheli, M.P. Mura, G. Grella, G. Esposito, B. Marchetti, E. Miele, M.S. Desole, M. Miele, P.A. Serra, Signaling pathways in the nitric oxide and iron-induced dopamine release in the striatum of freely moving rats: role of extracellular Ca^{2+} and L-type Ca^{2+} channels, *Brain Res.* 1047 (2005) 18–29.
- [21] P.A. Serra, G. Rocchitta, M.R. Delogu, R. Migheli, M.G. Taras, M.P. Mura, G. Esposito, E. Miele, M.S. Desole, M. Miele, Role of the nitric oxide/cyclic GMP pathway and extracellular environment in the nitric oxide donor-induced increase in dopamine secretion from PC12 cells, *J. Neurochem.* 86 (2003) 1403–1413.
- [22] J.P. Lowry, M. Miele, R.D. O'Neill, M.G. Boutelle, M. Fillenz, An amperometric glucose-oxidase/poly(*o*-phenylenediamine) biosensor for monitoring brain extracellular glucose: in vivo characterisation in the striatum of freely-moving rat, *J. Neurosci. Methods* 79 (1998) 65–74.
- [23] R. Moghimi, Ways to Optimize the Performance of a Differential Amplifier Application Note AN589, Rev. 0, Analog Devices Inc., 2002.
- [24] R.D. O'Neill, Long-term monitoring of brain dopamine metabolism in vivo with carbon paste electrodes, *Sensors* 5 (2005) 317–342.
- [25] C.P. McMahon, G. Rocchitta, S.M. Kirwan, S.J. Killoran, P.A. Serra, J.P. Lowry, R.D. O'Neill, *Biosens. Bioelectron.* 22 (2007) 1466–1473.

Biographies

Gaia Rocchitta has MSc in chemistry. In 2004, she received her PhD in neuroscience at Sassari University under the direction of Prof. M.S. Desole and Prof. E. Miele and the supervision of Mr. G. Esposito. She was awarded research fellowship in University College of Dublin (2004–2006). Her main research interests involve development of Glutamate biosensors and their application for in vivo detection of Glutamate in rats in physiological and pathological conditions.

Rossana Migheli is lecturer at Pharmacology Department in Sassari University, Medical School. Graduated with a MSc in pharmacy, she received her first PhD in pharmacology and toxicology and the second in neuroscience at Sassari University. Her main research interests are about the role of stem cells and neurochemicals in neurodegenerative diseases.

Sonia Dedola is graduated with a MSc in biology in 2004 at University of Sassari where is taking a PhD in neuroscience at Department of Pharmacology. She is studying in vitro neurochemistry of PC12 and stem cells using microdialysis and voltammetry and she is also developing microfluidic and microdialysis devices.

Giammaria Calia is graduated with a MSc in biology in 2004 at University of Sassari where is taking a PhD in neuroscience at Department of Pharmacology. He is involved in characterising neuronal stem cells studying morphology and behaviour; he is also involved in studying stem cells neurochemical responses to different pharmacological treatments oriented to PD therapy.

Maria Speranza Desole received her degree in 1971 at Sassari University. In 2001 became professor in pharmacology at Sassari University, Medical School. She was visiting professor at Dept. of Pharmacology, Medical College of Virginia (Richmond, Virginia, USA) in 1987, at Dept. of Pharmacology and Therapeutics, School of Medicine and Biomedical Sciences (SUNY at Buffalo, USA) in 1992, at Dept. of Experimental Therapeutics del Grace Cancer Drug Center (Roswell Park Cancer Institute, Buffalo, USA) in 1994, and Dept. of Molecular Physiology, Baylor College of Medicine (Houston, Texas, USA) in 1997. She is director of the Pharmacology Dept. at Sassari University, Medical School. At the moment her principal aim is focused in characterising morphology and behaviour of neuronal stem cells.

Egidio Miele is professor of pharmacology at Sassari University, Medical School. He became medical doctor receiving his degree at Napoli University in 1957. He was awarded a prestigious fellowship at Pharmacology Department in State University of New York collaborating with Nobel prize Dr. Robert F. Furchgott in 1966. His principal field of research is to study the role of ascorbic acid in protecting brain functions against several neurodegenerative diseases. At the moment his interest is focused on neurochemistry of neuronal stem cells.

John P. Lowry received his BSc in chemistry from University College Dublin (UCD) in 1988. He received his Ph.D in bioelectroanalytical chemistry from UCD under the direction of Prof. Robert D. O'Neill in 1992. Prior to his first academic appointment he was a Marie Curie Fellow at the University of Oxford where he worked in the University Laboratory of Physiology with Dr. Marianne Fillenz. He was appointed as a University Lecturer in Analytical Chemistry at the National University of Ireland, Maynooth (NUIM), in 1998. In 2004 he became a lecturer in pharmacology at the Conway Institute UCD and returned to NUIM in 2006 to take up the Chair of Chemistry. His research interests are in the area of bioanalysis particularly in the development, characterisation and application of sensor and biosensor systems for in vivo neurochemical monitoring.

Robert D. O'Neill, PhD, is professor of electrochemistry at UCD, Dublin, and a founding member of the Neuroanalytical Chemistry Laboratories

(www.naclgroup.org). He received his BSc in chemistry (1976) and PhD in electrochemistry (1980) from UCD, and was awarded research fellowships in Oxford University for postdoctoral studies in physiology and neurochemistry (1980–1985). Professor O'Neill's research program focuses on design and application of microsensors and biosensors for electrochemical monitoring of brain signalling systems.

Pier Andrea Serra is associate professor of pharmacology at University of Sassari, Medical School. He received his degree as medical doctor at Sassari Uni-

versity in 1998. He studied the in vivo Neurochemistry of Parkinson's Disease using microdialysis and voltammetry under the supervision of Dr. Maddalena Miele and received his PhD in pharmacology and toxicology from Sassari University in 2001. He worked as a Postdoctoral Fellow at University College of Dublin under the direction of Prof. Robert D. O'Neill and Prof. John P. Lowry. His main research interest involves the development and application of neuroanalytical techniques in order to study neurodegenerative diseases and stem cells metabolism (www.neuroscience.uniss.it).